Journal of Catalysis **189,** 456–462 (2000)
doi:10.1006/jcat.1999.2654, available online at http://www.idealibrary.com on IDEAL®

Genesis of Co/SiO_2 Catalysts: XAS Study at the Cobalt $L_{III,II}$ Absorption Edges

D. Bazin,* I. Kovács,† L. Guczi,† P. Parent,* C. Laffon,* F. De Groot,‡ O. Ducreux,§ and J. Lynch§

*LURE, Université Paris XI, Bât 209D, 91405, Orsay, France; †Department of Surface Chemistry and Catalysis, Institute of Isotope and Surface Chemistry, CRC HAS, P.O. Box 77, H-1525 Budapest, Hungary; ‡M.S.C., University of Groningen, Nijenborgh 4, 9747AG, Groningen, The Netherlands; and §Institut Français du Pétrole, 1 et 4 Avenue de Bois PrÈau, 92852, Rueil-Malmaison, France

Received March 1, 1999; revised June 28, 1999; accepted August 2, 1999

Silica-supported cobalt catalysts have been investigated by soft X-ray absorption techniques. Soft X-ray absorption spectra were collected at the Co $L_{II,III}$ edge during *in situ* reduction of calcined samples in a stream of hydrogen in the temperature range between 300 and 650°C. Using reference compounds, the structural transition occurring on Co_3O_4 clusters to give CoO species was established. Disappearance of the different features associated with Co^{2+} O_h symmetry was observed, probably due to disorder in the first coordination sphere of the cobalt atoms. For the interpretation of the spectra, numerical simulations based on the multiplet theory were carried out. Through these experiments we demonstrate the advantages of soft X-ray experiments in catalysis research involving 3d metals.

Key Words: **XAS study; genesis of Co/SiO_2 samples; reduction of Co_3O_4 and amorphous CoO.**

1. INTRODUCTION

The importance of cobalt-based catalysts in Fischer–Tropsch synthesis (1) has recently increased as new “gas-to-liquid” technologies such as the “Shell Middle Distillate” technology (2) and the high-efficiency EXXON process (3) have emerged. In addition to these processes, it has been shown that cobalt is also active in CH_4 conversion to higher hydrocarbons (4, 5) and the isomerization of hydrocarbons (6).

In order to prepare metallic cobalt particles with proper activity and stability, the precursor containing Co^{2+} ions must be reduced by H_2 (7). Large Co_3O_4 particles are easy to reduce completely to metallic Co^0 (8), but below a particle size of 6 nm the reduction of cobalt oxide is difficult. However, reducibility of Co^{2+} ions can be facilitated by increasing metal loading (9) or by addition of noble metals such as Pt (10–12), Ir (13), Rh (14–16), Ru (17), or Pd (18). In the case of NaY zeolite as support, the reducibility of cobalt is difficult even in the presence of platinum and ruthenium (19–24).

Enhancement in the reducible Co fraction facilitated by addition of a second metal is also generally associated with modification of the surface structure and with synergistic effect (25–28).

Although the reducibility of the ionic cobalt species was clearly demonstrated from the experiments cited above, the steps through which this process is progressing are not known. Because the techniques related to synchrotron radiation (X-ray absorption spectroscopy (XAS) (24, 29) or anomalous wide angle X-ray scattering (AWAXS) (30)) have been employed for two decades to determine structural parameters of poorly ordered materials at the atomic scale, these experimental techniques (30–33) can be utilised for *in situ* studies performed on mono- or multimetallic systems supported on inorganic oxides (34–36). Thereby correlation between the structure and catalytic activity can be established (37, 38).

Most of these results were obtained by using photons with energies around 10–20 KeV, corresponding either to the K edge of 3d (39) and 4d transition metals or to the L edge of 5d transition metals (40, 41). Since the energy range allows *in situ* studies, experiments can be performed either after (42) or during the chemical reaction (43).

Recent advances in theoretical background as well as in instrumentation have motivated several studies dedicated to the application of X-ray absorption spectroscopy at low energy (44–46), i.e., at the K edge of light elements (47) or at the L edge of 3d transition metals. For example, in the case of mineral compounds the usefulness of 2p ($L_{II,III}$) X-ray absorption spectroscopy has been demonstrated (48).

In this paper we report soft X-ray absorption experiments performed on supported cobalt catalysts. The objective is to show how fine spectral features at Co L_{III} and Co L_{II} edges can be employed to describe the electronic state of the cobalt metal. This new probe not only allows us to recognise the valence states of 3d ions but also provides site symmetry information. Soft X-ray absorption spectra collected after *in situ* reduction under hydrogen at different temperatures between 300 and 650°C feature also structural disorder in the first coordination sphere of the cobalt.

0021-9517/00 $35.00

2. EXPERIMENTAL

2.1. *Catalyst Preparation*

A silica-supported cobalt catalyst with 13 wt% cobalt loading was studied. The samples were prepared by incipient wetness on silica support type W.R. Grace, the specific surface area being 460 m^2/g using aqueous solution of Co(NO$_3$)$_3$ 6H$_2$O. The sample was dried for 2 h at 100°C, calcined for 3 h at 600°C, and then characterised by XRD (Cu $K\alpha$) and by classical X-ray absorption spectroscopy at the Co K edge. Large clusters of Co_3O_4 (above 15 nm) were detected by XRD. The sample was therefore named "Co_3O_4"/SiO$_2$. A part of this sample was reduced in a stream of hydrogen (temperature ramp 2°C/min to 450°C followed by an isothermal period of 2 h), then passivated by slow exposure to air by allowing air to leak into the reaction chamber overnight. Then the sample was saturated with distilled water, dried again, and calcined at 600°C for 4 h. This latter sample appeared amorphous in XRD studies and was named α-Co/SiO$_2$ (49). A phase close to Co_2SiO_4 was identified from the analysis of EXAFS oscillations beyond the cobalt K edge (8).

2.2. *NEXAFS Experiments*

Co L edge spectra were collected at the LURE synchrotron facility in Orsay using the synchrotron radiation from the SACO storage ring running at 800 MeV with an average current of 300 mA and a lifetime of 10 h. The beam line (SACEMOR) placed after a bending magnet is equipped with a high-resolution Spherical Mirror-Plane Grating Monochromator (S. M.-P. G. M. 12 m).

The monochromator resolution was about 0.15 eV (FWHM) for the cobalt L$_{III}$ edge. Beam dimensions were about 0.5 mm × 0.2 mm at the sample, and the pressure in the analyser chamber was directly related to the vacuum in the synchrotron ring.

Powdered samples (10–20 mg) were mounted on a clean sample holder plate, by allowing a drop of suspension of the powder in acetone to dry on the sample holder, and were oriented with the sample surface at 45° to the beam. Soft X-ray absorption spectra have also been collected after a chemical treatment in an *in situ* furnace implemented on the beam line. The samples were transferred into the preparation chamber for heating in vacuum (1–2×10^{-8} Pa) or reduction in hydrogen (1×10^{-4} Pa). More precisely, at the beginning the pressure in the sample preparation chamber is 10^{-8} Pa. Then, we introduce hydrogen while the vacuum devices are still working, so the pressure of the sample preparation chamber increases up to 10^{-6} Pa. This value of the pressure is maintained for 30 min.

The absorption spectra were recorded in total electron yield mode and were corrected for beam intensity variations during measurements; the intensity of the beam was measured via the photoemission of a gold grid (50). Data were normalised and calibrated as in previous work (45, 51).

3. RESULTS

3.1. *Measurements of Reference Compounds (CoO, Co$_2$SiO$_4$, and Co$_3$O$_4$)*

The L edge spectra can be divided into two parts, L$_{III}$ and L$_{II}$ dominated by the respective 2p$_{3/2}$ and 2p$_{1/2}$ characters of the core hole. In Fig. 1 the Co 2p X-ray absorption spectra of the reference compounds, namely, CoO, Co_2SiO_4, and Co_3O_4, are presented. Large variations of spectral features are clearly visible in the fine structure at the edges.

(i) The spectrum of CoO is similar to that found in previous measurement (51). This reference material was obtained from Co_3O_4 after heating at 500°C for 10 h under high vacuum. At this point it is important to note that the ground state of this compound is described as a single configuration of 3d^7 character corresponding to a $^4T_{1g}$ ground term (8).

(ii) The Co L$_{III}$ and Co L$_{II}$ edges in the spectra of CoO and Co_2SiO_4 reference compounds are very similar. This indicates that the valence states of the cobalt atoms as well as the symmetries of the sites are the same, a result in line with the crystallography. In both cases, Co^{2+} ions

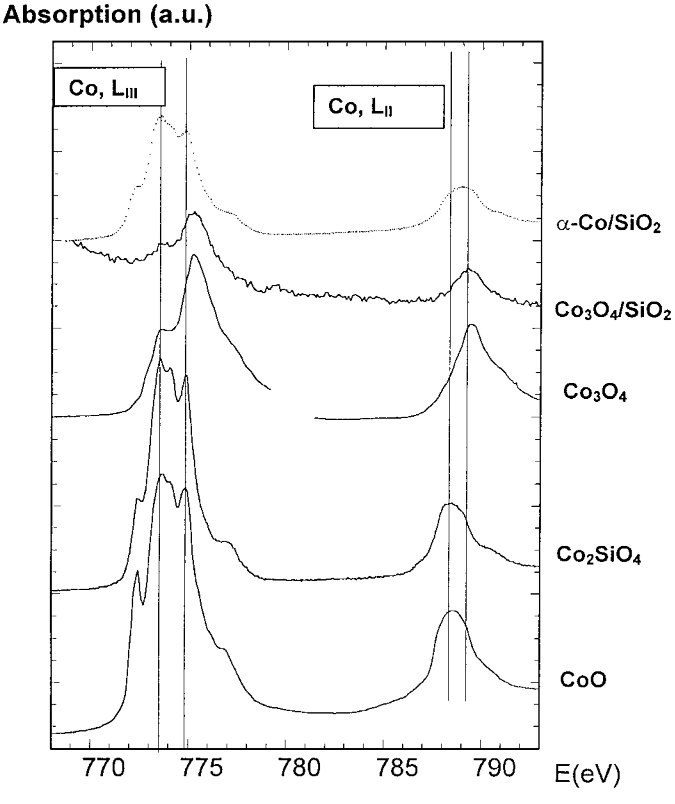

FIG. 1. Normalised Co L$_{III,II}$ edge spectra of Co_3O_4, CoO, and Co_2SiO_4, as well as the "Co_3O_4"/SiO$_2$ and α-Co/SiO$_2$ catalysts.

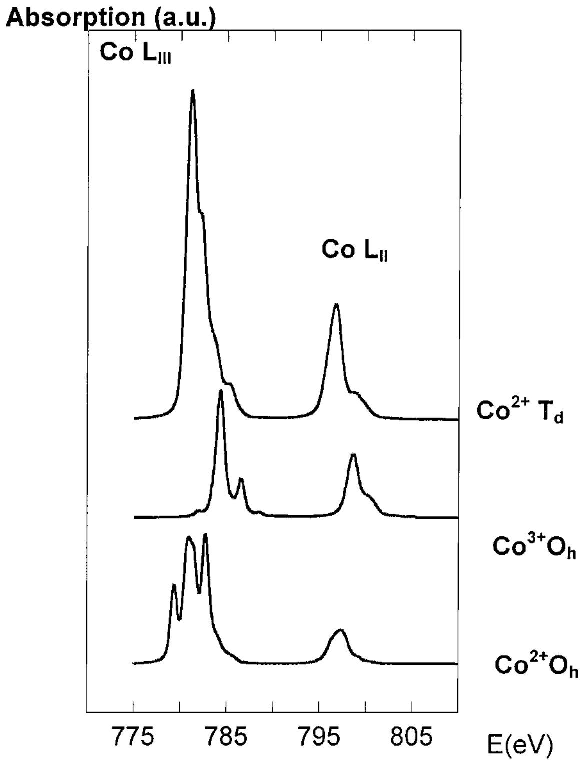

FIG. 2. Numerical simulations using the multiplet theory for cobalt.

are octahedrally coordinated to oxygen anions ($N=6$, R (Co–O) $= 0.213$ nm for CoO (8) and for Co_2SiO_4 there are two slightly different oxygen positions $N=3.5$, $R=0.208$ nm; $N=2.5$, $R=0.22$ nm (8)).

(iii) Finally, for Co_3O_4 the spectrum is a combination of Co^{2+} (T_d) ($N=4$, $R=0.191$ nm) and Co^{3+} (O_h) ($N=6$, $R=0.1956$ nm) (8).

The recent advances in theoretical background related to soft X-ray experiments have motivated a set of numerical simulations (52), shown in Fig. 2, corresponding to the configurations of Co^{2+} T_d, Co^{3+} O_h, and Co^{2+} O_h. These calculations show the great sensitivity of 2p spectroscopy to the valence state of the cobalt atoms as well as to the symmetry of the sites. In order to simulate the Co $L_{III,II}$ spectra of Co_3O_4, a simple linear combination of the components can be used. Note that the exact position of these spectra vs photon energy is not exactly determined from theory.

3.2. Catalysts in As-Received State ("Co_3O_4"/SiO_2 and α-Co/SiO_2)

The Co $L_{III,II}$ edges of the "Co_3O_4"/SiO_2 catalyst are shown in Fig. 1. This spectrum is consistent with our previous results obtained at the Co K edge, suggesting that this cobalt-based catalyst contains large Co_3O_4 particles. The Co L_{III} edge is very similar to the spectra obtained for the Co_3O_4 reference compound. For this catalyst it is clear that Co atoms are in both the Co^{2+} (T_d) and the Co^{3+} (O_h) electronic state.

The Co L_{III} edge of the α-Co/SiO_2 catalyst looks very similar to that of Co_2SiO_4 (or CoO). Thus, cobalt atoms are mainly in the Co^{2+} ionic state, the symmetry of the first oxygen coordination sphere being octahedral. Nevertheless, the position of the L_{II} energy clearly differs from that of the Co L_{II} edge in the reference compounds Co_2SiO_4 and CoO. In fact, the shape of this feature (a broadening to the right side is observed) seems to indicate the presence of some Co_3O_4 clusters.

3.3. In Situ Reduction of the α–Co/SiO_2 Sample

The cobalt absorption spectra after *in situ* calcination and then after *in situ* reduction in a stream of H_2 at different temperatures for the α-Co/SiO_2 sample are plotted on Figs. 3 and 4 for the Co L_{III} and Co L_{II} edges, respectively. An increase in the temperature up to 350°C under vacuum, is sufficient to modify the Co L_{III} edge (Fig. 3). The features assigned to the Co_3O_4 clusters disappear, probably due to the formation of CoO-type clusters. After reduction under H_2 at 500°C for 30 min the Co L_{III} edge has a similar shape and position as those of the Co_2SiO_4 and CoO samples. A

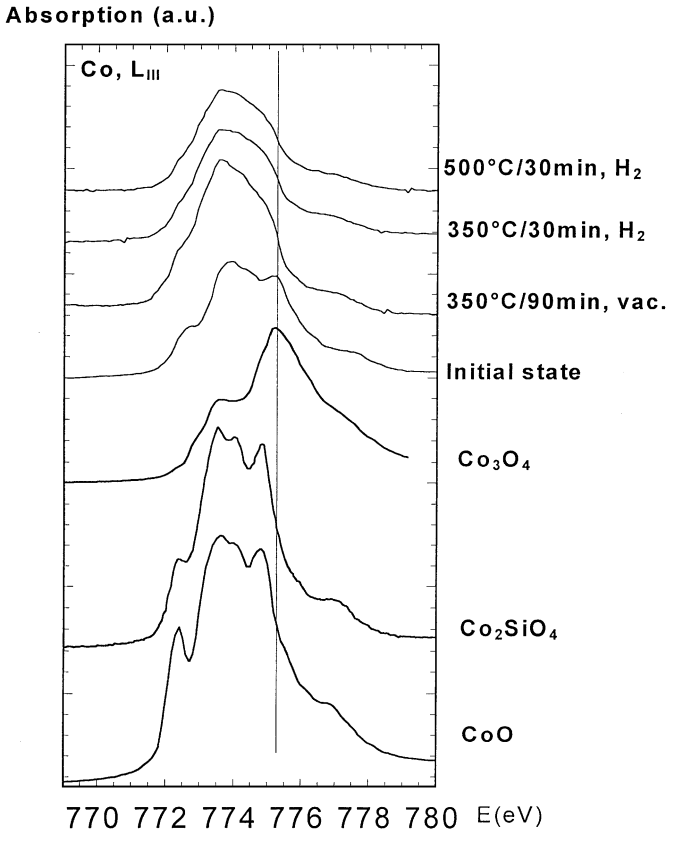

FIG. 3. Evolution of the cobalt L_{III} edge during reduction under hydrogen at different temperatures for the α-Co/SiO_2 catalyst.

striking point is the lack of fine details in the Co L$_{III}$ edge. Unless the symmetry of the Co^{2+} ions is altered, one possible explanation for the loss of these features is a disorder of the first coordination sphere around the cobalt atoms.

As far as the Co L$_{II}$ edge is concerned (Fig. 4), the first transformation observed after heating the sample under vacuum is well observed. The shift of the Co L$_{II}$ edge toward lower energy is in line with the disappearance of Co$_3$O$_4$ clusters or more precisely with the disappearance of the Co^{3+} O$_h$ species. The reduction under hydrogen at 350°C and then at 500°C does not significantly modify the position or the shape of the Co L$_{II}$ edge. It seems that the Co L$_{II}$ edge is less sensitive to structural changes than the Co L$_{III}$ edge.

3.4. *In Situ Reduction of the "Co$_3$O$_4$"/SiO$_2$ Sample*

In the "Co$_3$O$_4$"/SiO$_2$ sample (Figs. 5 and 6), the first reduction under H$_2$ at 300°C seems to change the local ordering around the cobalt atoms. The fact that the amplitude of the first feature increases indicates that a silicate or CoO like phase may be formed. This modification continues under the reduction at 500°C, and finally, after reduction at 650°C (30 min, H$_2$), the phase transition is almost completed at the end of the process as indicated by the top spectrum of Fig. 6. Even if the signal-to-noise ratio is poor, we have to underline that in the case of this sample detailed structure is observed at the Co L$_{III}$ edge.

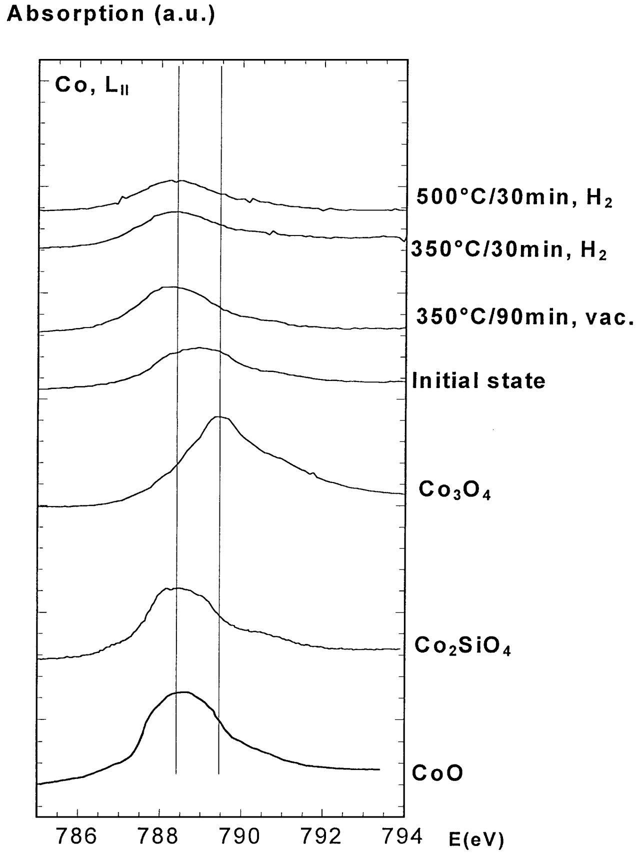

FIG. 4. Evolution of the cobalt L$_{II}$ edge during reduction under hydrogen at different temperatures for the α-Co/SiO$_2$ catalyst.

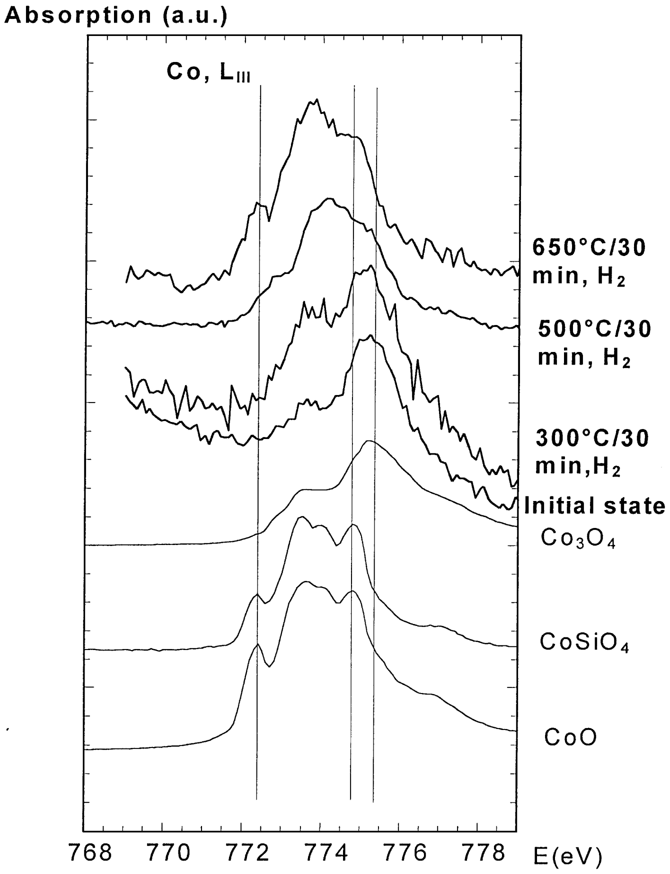

FIG. 5. Evolution of the cobalt L$_{III}$ edge during reduction under hydrogen at different temperatures for the catalyst "Co$_3$O$_4$"/SiO$_2$.

Finally, we have to underline that cobalt atoms are not reduced at this temperature, and work is in progress to understand the influence of the low pressure (10^{-4} Pa H$_2$) on the reduction process.

4. DISCUSSION

The new approach demonstrated here clearly shows a possibility offered by soft X-ray spectroscopy for the study of real heterogeneous catalysts in powdered form. The results illustrate that during pretreatment (e.g., calcination, reduction) of a sample important structural information can be obtained regarding the disorder of the first coordination sphere of the metal species deposited on a support.

The advantages and limitations of probing structural and electronic states through the K and L edges of 3d transition metals can be discussed through a comparison of the theoretical formalism associated with each absorption edge. For the numerical simulation of the L edge, the theoretical approach using multiplets is based on the evaluation

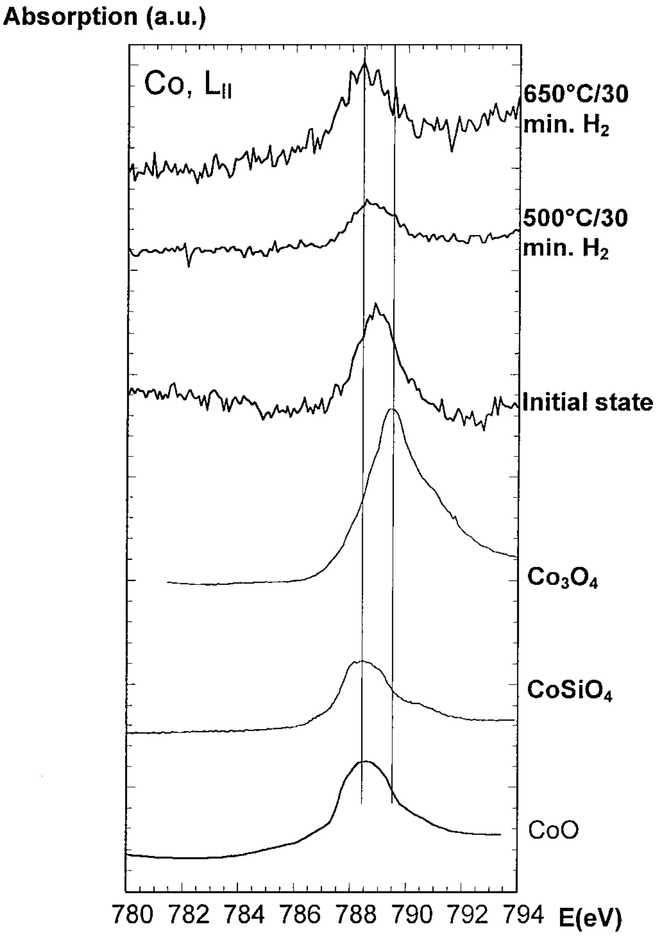

FIG. 6. Evolution of the cobalt L_{II} edge during reduction under hydrogen at different temperatures for the catalyst "Co_3O_4"/SiO_2.

of dipole transitions, basically ignoring the details of the electron scattering processes. Thus, the L-edge calculation is quasi-atomic, only the symmetry breaking from atomic to cubic or to octahedral, due to the neighbouring oxygen atoms, is important and not the exact atomic positions. Also note that a crucial extra ingredient with respect to multiple scattering is the large overlap between the core and valence wave functions.

In multiple scattering (K edge), the calculation is concerned with the scattering of the emitted electron. Full multiple scattering calculations can be performed using the CONTINUUM (53) or the FEFF code (54), and both methods are based on the same physics with two different mathematical expressions. In the FEFF mode, the oscillations are expressed as a sum of different multiple scattering contributions. Another difference comes from the lifetime of the excited state. The high K-edge energy compared to that of the L edge implies that detailed features at the edges can best be observed in the case of a soft X-ray experiment, while the shoulder generally measured at the K edge can be observed in fine details at the L edge. Thus, the data analysis process can be more effective at the L edge.

We can also compare this soft X-ray approach to the more conventional ELNES technique (Energy Loss Near Edge Structure) (55). In a previous study the ELNES of a set of reference oxides was used as a fingerprint (56). The spectrum of Co_3O_4 illustrates one major limitation of this electron-related technique. By increasing the number of energy scans to improve the signal-to-noise ratio, the Co $L_{III,II}$ profile is modified through a reduction of part of the Co^{3+} species.

The diffuse reflectance spectroscopy (DRS) (57) can also be used to characterise catalysts since it is a simple and inexpensive method that can give the same sort of information. Recently, a study of the local structure of molybdenum–magnesium binary oxides by means of Mo L_{III} edge Xanes and UV-vis spectroscopy has been performed (58). The results obtained by UV-vis spectra are in accordance with that of the L_{III} XAFS study but not with the studies of Mo K-edge XAFS and XRD. The authors concluded that the information obtained by UV-vis spectra is more sensitive to the surface structure than that of Mo K-edge XAFS spectra. Recently, a comparison between UV-vis and EXAFS has been done regarding the coordination of Ni^{2+} ions to lattice oxygen in calcined faujasite-type zeolites (59). The authors point out the limitation of the DRS analysis technique, which appears to be more sensitive to low-symmetry species. More precisely, in hydrothermally synthesised CoAPO-5 with cobalt content $x < 2.5 \times 10^{-4}$, the Co^{2+} ions surrounded by oxygen atoms are found to be in a tetrahedral environment. For high cobalt loading, most of the Co^{2+} ions are in extra-lattice positions (O_h), in contrast to the results given by DRS, which indicate that Co^{2+} ions are only in tetrahedral symmetry.

The analogy between UV-vis and XANES is obvious if the role of the electron transition from the filled orbital to the empty state around the central ions is concerned. The differences between the techniques are as follows:

(i) By UV-vis the crystal field splitting of the electron shell around the central ion can be directly measured within a few eV.

(ii) In soft X-ray absorption the empty states in the energy scale can be determined. The energy difference is in a range 100 times higher. Interference of the photoelectrons with the next coordination sphere becomes important because the wavelength of the photoelectrons is in the range of a few nm. Diffraction makes the interpretation more difficult.

(iii) By the soft X-ray absorption spectra the genesis of the transformation of Co_3O_4 to CoO can be followed and the oxidation states and coordination can be simultaneously determined.

Finally, regarding the data analysis process, we have already pointed out that for nanometer-scale materials, it is not possible to simulate the XANES part for K-edge with a linear combination of the XANES of well-crystallised reference compounds (60). In some particular cases, and more precisely in the case of nanometer scale metallic copper clusters, ab initio calculations have clearly pointed out that a 13-atom environment is not enough to produce all the features present at the K edge of the metallic copper foil. Thus the XANES part can be used as a fingerprint of the cluster size.

As has been remarked above, the L-edge calculations are quasi-atomic. Thus, even in the case of nanometer-scale materials and more generally poorly ordered compounds, it is possible to simulate the XANES part of the Co L-edge through a linear combination of the XANES of well-crystallised reference compounds. This advantage is very important because nanometer scale entities are at the core of numerous chemical processes (61–65). The fact that such a simple data analysis can be performed implies more significant structural and electronic results. The interpretation of the soft X-ray absorption spectra is easy if the reference compounds are known, and the structure of the real samples can be fitted simply by addition of the spectra of the two corresponding Co^{2+} and Co^{3+} (O_h) models.

In the case of our catalysts, soft X-ray experiments act as a phase sensitive technique, the different details observed at the Co L_{III} edge being used as a fingerprint of the different phases included in the material. This is clearly the case for α-Co/SiO$_2$. If the Co L_{III} edge looks very similar to that of Co_2SiO_4 (or CoO), the shape and the position of the Co L_{II} edge indicate the presence of Co_3O_4 clusters. Because this approach can be applied to poorly ordered materials whereas X-ray diffraction is dedicated to well-crystallized compounds, it can be considered as a useful tool in heterogeneous catalysis research. Finally, the possibility of performing *in situ* experiments enables a real improvement in the knowledge of the structural evolution of the material in reaction conditions.

5. CONCLUSION

In many research fields, including catalysis, advances in theoretical background as well as in instrumentation have transformed soft X-ray spectroscopy into a key research tool. The theoretical results associated with a set of data collected on a real catalysts, clearly show the importance of 2p ($L_{III,II}$) X-ray absorption spectroscopy as an element-specific valence probe. This new approach provides site symmetry information for each ion site.

The results obtained on reference compounds and supported catalysts show that fine details measured at the Co L_{III} edge can be used as a fingerprint of the different phases present in the material.

Moreover, the blurring of details in the Co L_{III}-edge absorption spectra gives an indication of structural disorder in the first coordination sphere of the cobalt atoms. Here, we arrive at the limit of the theoretical formalism currently used in the analysis of transition metal L-edge absorption. The significant information gained from this particular result can be utilised to link structural characteristics to the catalytic activity, in addition to being a challenge for theoretical physics.

REFERENCES

1. Dry, M. E., *in* "Catalysis Sciences and Technology" (J. R. Anderson and M. Boudart, Eds.), Vol. 1, p. 159. Springer Verlag, Berlin, 1981.
2. van Wechem, V. M. H., and Senden, M. M. G., *in* "Natural Gas Conversion II" (H. E. Curry-Hyde and R. F. Howe, Eds.), Stud. Surf. Sci. Catal., Vol. 81, p. 43. Elsevier, Amsterdam, 1994.
3. Eisenberg, B., Fiato, R. A, Mauldin, C. H., Say, G. R., and Soled, S. L., "Natural Gas Conversion V" (A. Parmaliana, D. Sanfilippo, F. Frusteri, A. Vaccari, and F. Arena, Eds.), Stud. Surf. Sci. Catal., Vol. 119, p. 943. Elsevier, Amsterdam, 1998.
4. Koerts, T., and van Santen, R. A., *J. Mol. Catal.* **70**, 119 (1990).
5. Guczi, L., Sarma, K. V., and Borkó, L., *J. Catal.* **167**, 495 (1997).
6. Garin, F., Girard, P., Maire, G., Lu, G., and Guczi, L., *Appl. Catal. A* **152**, 237 (1997).
7. Keim, W., Ed., "Catalysis in C1 Chemistry." Reidel, Dordrecht, 1983.
8. Khodakov, A., Lynch, J., Bazin, D., Rebours, B., Zanier, N., Moisson, B., and Chaumette, P., *J. Catal.* **68**, 16 (1997).
9. Zsoldos, Z., Garin, F., Hilaire, L., and Guczi, L., *Catal. Lett.* **33**, 39 (1995).
10. Zsoldos, Z., Hoffer, T., and Guczi, L., *J. Phys. Chem.* **95**, 798; Zsoldos, Z., Hoffer, T., Guczi, L., Zyade, S., Maire, G., and Garin, F., *J. Phys. Chem.* **95**, 802 (1991).
11. Dees, M. J., Shido, T., Iwasawa, Y., and Ponec, V., *J. Catal.* **124**, 530 (1990).
12. Zsoldos, Z., Garin, F., Hilaire, L., and Guczi, L., *J. Mol. Catal. A* **111**, 113 (1996).
13. Esteban Puges, P., Garin, F., Maire, G., Weisang, F., Bernhardt, P., Girard, P., Guczi, L., and Schay, Z., *J. Catal.* **114**, 153 (1988).
14. Van't Blik, H. F. J., and Prins, R., *J. Catal.* **97**, 188 (1986).
15. Martens, J. H. A., Van't Blik, H. F. J., and Prins, R., *J. Catal.* **97**, 200 (1986).
16. Van't Blik, H. F. J., Koningsberger, D. C., and Prins, R., *J. Catal.* **97**, 210 (1986).
17. Guczi, L., Sarma, K. V., Koppány, Zs., Sundarajan, R., and Zsoldos, Z., *in* "Natural Gas Conversion IV" (M. de Pontes, R. L. Espinoza, C. P. Nicolaides, J. H. Scholz, and M. S. Scurrell, Eds.), Stud. Surf. Sci. Catal., Vol. 107, p. 333. Elsevier, Amsterdam, 1997.
18. Sárkány, A., Zsoldos, Z. Stefler, G. Hightower, J. W., and Guczi, L., *J. Catal.* **157**, 179 (1995); Guczi, L., Schay, Z., Stefler, G., and Mizukami, F., *J. Mol. Catal. A*. **141**, 177 (1999).
19. Lu, G., Hoffer, T., and Guczi, L., *Catal. Lett.* **14**, 207 (1992).
20. Zhang, Z., and Sachtler, W. M. H., *J. Chem. Soc. Faraday I* **86**, 2313 (1990).
21. Guczi, L., Sundararajan, R., Koppány, Zs., Zsoldos, Z., Schay, Z., Mizukami, F., and Niwa, S., *J. Catal.* **167**, 482 (1997).
22. Yin, Y.-G., Zhang, Z., and Sachtler, W. M. H., *J. Catal.* **138**, 721 (1992).
23. Guczi, L., Koppány, Zs., Sarma, K. V., Borkó, L., and Kiricsi, I., *in* "Progress in Zeolite and Microporous Materials" (H. Chon, S.-K. Ihm, Y. S. Uh, Eds.), Stud. Surf. Sci. Catal., Vol. 105, p. 861. Elsevier, Amsterdam, 1997.
24. Moller, K., and Bein, T., *in* "Zeolites: Facts, Figures, Future" (P. A. Jacobs and R. A. van Santen, Eds.), Stud. Surf. Sci. and Catal., Vol. 49, p. 985. Elsevier, Amsterdam, 1989.
25. Iglesia, E., Soled, S. L., and Fiato, R. A., *J. Catal.* **137**, 212 (1992).

26. Xiao, F.-S., Fukuoka, A., and Ichikawa, M., *J. Catal.* **138**, 206 (1992).
27. Iglesia, E., Soled, S. L., Fiato, R. A., and Via, G. H., *J. Catal.* **143**, 345 (1993).
28. Kogelbauer, A., Goodwin, J. G., and Okachi, R., *J. Catal.* **160**, 125 (1996).
29. Stern, E. A., Sayers, D. E., and Lytle, F. W., *Phys. Rev. B* **11**, 4836 (1975).
30. Materlik, G., Sparks, C. J., and Fisher, K., Eds., "Resonant Anomalous X-Ray Scattering." North Holland, Amsterdam, 1994.
31. Bazin, D., Sayers, D., and Rehr, J., *J. Phys. Chem. B* **101**, 11040 (1997).
32. Clausen, B. S., Grabaek, L., Steffensen, G., Hansen, P. L., and Topsoe, H., *Catal. Lett.* **20**, 23 (1993).
33. Coyler, L. M., Greaves, G. N., Carr, S. W., and Fox, K. K., *J. Phys. Chem. B* **101**, 10105 (1997).
34. Bazin, D., Sayers, D., Rehr, J. J., and Mottet C., *J. Phys. Chem. B* **101**, 5332 (1997).
35. Gutzmann, V., and Vogel, W., *J. Phys. Chem.* **94**, 4991 (1990).
36. Bazin, D., and Sayers, D., *Jpn. J. Appl. Phys.* **32**, 252 (1993).
37. Guyot-Sionnest, N. S., Villain, F., Bazin, D., Dexpert, H., Lynch, J., and Lepeltier, F., *Catal. Lett.* **8**, 283 (1991).
38. Guyot-Sionnest, N. S., Villain, F., Bazin, D., Dexpert, H., Lynch, J., and Lepeltier, F., *Catal. Lett.* **8**, 297 (1991).
39. Barrett, P. A., Sankar, G., Jones, R. H., Catlow, C. R., and Thomas, J. M., *J. Phys. Chem.* **101**, 9555 (1996).
40. Bazin, D., Dexpert, H., Guyot-Sionnest, N. S., Bournonville, J. P., and Lynch, J., *J. Chim. Phys.* T86, **718**, 1707 (1989).
41. Prins, R., and Koningsberger, D. C., "X-Ray Absorption: Principles, Applications, Techniques of Exafs, Sexafs and Xanes." Wiley, New York, 1988.
42. Esteban, P., Conesa, J. C., Dexpert, H., and Bazin, D., *in* "Spectroscopic Analysis of Heterogeneous Catalysts" (J. L. G. Fierro, Ed.). Elsevier, Amsterdam, 1992.
43. Bazin, D., Dexpert, H., and Lynch, J., *in* "X-Ray Absorption Fine Structure for Catalysts and Surfaces" (Y. Iwasawa, Ed.). World Scientific, Singapore, 1996.
44. Chen, J. G., *Surf. Sci. Report* **30**, 1 (1997).
45. De Groot, F. M. F., *J. Electron Spectrosc. Relat. Phenom.* **67**, 529 (1994).
46. Charnock, J. M., Henderson, C. M. B., Mosselmans, J. F. W., and Pattrick, R. A. D., *Phys. Chem. Min.* **23**, 403 (1996).
47. Okajima, T., Teramoto, K., Mitsumoto, R., Oji, H., Yamamoto, Y., Mori, I., Ishii, H., Ouchi, Y., and Seki, K., *J. Phys. Chem. A* **102**, 7093 (1998).
48. Cressey, G., Henderson, C. M. B., and van der Laan, G., *Phys. Chem. Min.* **20**, 111 (1993).
49. Khodakov, A., Ducreux, O., Lynch, J., Rebours, B., and Chaumette, P., *Oil Gas Sci. Technol.* **54**(4) (1999).
50. Parent, Ph., Laffon, C., Tourillon, G., and Cassuto, A., *J. Phys. Chem.* **99**, 5058 (1995).
51. van Elp, M., Wieland, J. L., Eskes, H., Kuiper, P., and Sawatzky, G. A., *Phys. Rev. B* **44**, 6090 (1991).
52. De Groot, F. M. F., Abbate, M., van Elp, M., Sawatzky, G. A., Ma, Y. J., Chen, C. T., and Sette, F., *J. Phys. Cond. Mater.* **5**, 2277 (1993).
53. Natoli, C. R., Misemer, D. K., Doniach, S., and Kutzler F. W., *Phys. Rev. A* **22**, 1104 (1980).
54. Rehr, J. J., and Albers R. C., *Phys. Rev. B* **41**, 8149 (1990).
55. Ekardt, W., and Tran Thoai, D. B., *Solid State Commun.* **45**, 1083 (1983).
56. Szymansky, R., Payen, E., *in* "Proceedings, 2nd European Conference on Progress in X-Ray Synchrotron Radiation Research," Vol. 25, SIF, Bologna, 1990.
57. Garbowski, E., Kodratoff, Y., Mathieu, M. V., and Imelik, B., *J. Chim. Phys. Chim. Biol.* **69**, 1386 (1972).
58. Aritani, H., Tanaka, T., Funabiki, T., Yoshida, S., Eda, K., Sotani, N., Kudo, M., and Hasegawa, S., *J. Phys. Chem.* **100**, 19495 (1996).
59. Lepetit, C., and Che, M., *J. Phys. Chem.* **100**, 3137 (1996).
60. Bazin, D., Bensaddik, A., Briois, V., and Saintavict, Ph., *J. Phys.* **C4–6**, 481 (1996).
61. De Bont, P. W., Vissenberg, M. J., De Beer, V. H. J., van Veen, J. A. R., van Santen, R. A., and van der Kraan, A. M., *J. Phys. Chem. B* **102**, 3072 (1997).
62. Barrett, P. A., Sankar, G., Catlow, C. R., and Thomas, J. M., *J. Phys. Chem.* **100**, 8977 (1996).
63. Scheuring, E. M., Calvin, W., Wirt, M. D., Miller, L. M., Fischetti, R. F., Lu, Y., Mahoney, N., Xie, A., Wu, J. J., and Chanc, M. R., *J. Phys. Chem.* **100**, 3344 (1996).
64. O'Day, P. A., Chisholm-Brause, C. J., Towle, S. N., Parks, J., and G. A., Brown, G. E., *Geochim. Cosmochim.* **60**(14), 2515 (1996).
65. Leliveld, B. R. G., van Dillen, J. A. J., Geus, J. W., Koningsberger, D. C., and de Boer, M., *J. Phys. Chem. B* **101**, 11160 (1997).